Three-Dimensional Numerical Study of Flow Characteristics Through a Centrifugal Pump

Dr. Jalal M. Jalil*

Dr. Khalaf H. Ali**

Dr. Hussein M. al-Yassiri*

***Department of Mechanical Engineering**
University of Technology
****Technical College of Mosul**

Abstract

A solution method is developed to obtain three-dimensional velocity and pressure distribution within a centrifugal pump impeller. The method is based on solving fully elliptic partial differential equations for the conservation of mass and momentum by finite difference method to convert them into algebraic equations. The effect of turbulence introduced using a certain algebraic model based on modified Prandtl's mixing length theorem. The conical coordinate system is used in order to fit an arbitrary hub-to-shroud shape. The set of algebraic equations is solved simultaneously by "SIMPLE" algorithm to obtain velocity and pressure distribution within the impeller passage. The results are compared with previous experimental results of other researcher under the same operating circumstances and acceptable agreement has been found.

Key Words: Numerical Analysis, centrifugal Pump, Performance, Flow Analysis.

دراسة عددية ثلاثية الابعاد لاداء الجريان خلال مضخة الطرد المركزي

الدكتور جلال محمد جليل*

الدكتور خلف حسن علي**

الدكتور حسين مجيد الياسري*

* قسم الهندسة الميكانيكية / الجامعة التكنولوجية – ** قسم التبريد والتكييف/ الكلية التقنية في الموصل

الخلاصة

تم تطوير طريقة حل عددية لمعرفة التوزيع الثلاثي الأبعاد للسرعة والضغط خلال دافعة مضخة الطرد المركزي . وقد اعتمدت الطريقة على حل المعادلات التفاضلية الجزئية لحفظ

الكتلة والزخم (conservation of both mass and momentum) بواسطة استخدام طريقة الفرو قات المحـــددة (finite difference method) لتحويلها إلى معادلات جبرية.تم استخدام مود يل جبري يعتمد على نظرية براندتل للطول المختلط المعدلة (modified Prandtl's mixing length theorim) لتعريف تأثير الاضطراب.وقد تم استخدام نظام الإحداثي المخروطي (conical coordinate system) لكي يناسب أي شكل عشوائي لسطح مقطع الدافعة (hub-to-shroud surface).تم حل مجموعة المعادلات الجبرية في وقت واحد بطريقة ("SIMPLE" algorithm) لمعرفة توزيع السرعة والضغط عبر ممر الدافعة. تمت مقارنة النتائج مع نتائج عملية لباحث آخر تحت نفس ظروف التشغيل ,وقد بينت المقارنة توافقية مقبولة.

Nomenclatures **Units**

Received 3 March 2006 **Accepted 19 April 2007**

a_j : Coefficient for grid point. [kg.m^{-3}.s^{-1}]

a_E, a_W, a_S, a_N, a_B, a_F : Coefficients for neighboring grid points. [kg.m^{-3}.s^{-1}]

b,b_1: source term .

f : Factor accounts for effects of curvature and rotation on turbulent viscosity Equation (5).

l : Mixing length. [m]

n: Distance measured towards nearest wall. [m]

P: Pressure. [N.m^{-2}]

P_o: Static pressure at the center of the inlet section. [N.m^{-2}]

P.S: Pressure side.

r: Radius coordinate in the conical coordinate system [m]

r_o: Radius of the passage exit. [m]

R : Distance of a coordinate point (ϕ , r, θ) from the axis of rotation. [m]

S.S: Suction side.

U_2: Peripheral speed at the passage exit. [m.s^{-1}]

u : Velocity component in the ϕ - direction. [m.s^{-1}]

v : Velocity component in the r - direction. [m.s^{-1}]

w : Velocity component in the θ - direction. [m.s^{-1}]

z : Distance along impeller passage from inlet. [m]

Φ : General form of the dependent variable. [rad]

θ, ϕ : Angular coordinate in conical coordinate system. [rad]

μ_{eff} : The effective viscosity. [kg.m^{-1}.s^{-1}]

μ_L : The laminar viscosity. [kg.m^{-1}.s^{-1}]

μ_t: The turbulent viscosity. [kg.m^{-1}.s^{-1}]

ρ : Density. [kg.m^{-3}]

ψ : Coefficient of pressure head $(p-p_o)/ (\rho U_2^2/2)$.

Ω : Angular velocity of the impeller. [rad.s^{-1}]

1. Introduction

A focal point of research in turbomachinery flow problems has been the development of suitable solution methods to the flow field inside these machines. In the past few years extensive progress has been made in the application of different solution techniques. Nevertheless, general flow solutions within turbomachine passages presently remain mostly beyond the scope of prevailing methods.

Murakami et al., [1] reported an experimentally three-dimensional velocity and pressure distributions in the impeller passage of centrifugal pump. Zhang and Assains [2] presented a segregated approach for the prediction of three-dimensional, compressible, subsonic flows. The method uses a collocated finite volume scheme in body-fitted coordinates to solve Navier-Stokes equations with state equations. The ability of the method to perform satisfactorily near the low Mach number limit is demonstrated through comparisons with incompressible flow measurements. Polititis and Giannakoglou [3] solved the steady state Navier-Stokes equations in transonic flows using an elliptic formulation. A staggered solution algorithm was established. The momentum equations were solved in terms of the permitive variables, while the pressure correction was used to update both the convection mass flux components and the pressure itself. Turbulence was resolved through the $(k-\varepsilon)$ model. Dealing with turbomachinery applications, results were presented in two-dimensional compressor and turbine cascades under design and off design conditions. The predicted results were in very good agreement with the measurements. Wang and Komori [4] extended a pressure based finite volume method (was originally developed to predict incompressible flow) to predict the unsteady three-dimensional compressible flow within a centrifugal impeller. The general curvilinear coordinate system was used, and the collocated grid arrangement was adopted. The standard $(k-\varepsilon)$ model was implemented to model the turbulence effects. The procedure was successfully applied to predict various compressible subsonic and supersonic flows. Hofmann and Stoffel [5] presented a special test-pump with 2D curvature blade geometry in cavitating and non-cavitating conditions using different experimental techniques and a 3D numerical model of cavitating flows. Experimental and numerical results concerning pump characteristics and performance breakdown were compared at different flow conditions. Appearing types of cavitation and the spatial distribution of flow within the runner were also analyzed. Mununga at al., [6] presented numerical simulations of the flow field generated by a six-bladed paddle impeller in a closed unbaffled mixing vessel. Computations were performed using the CFD software package FLUENT using grid generated from the pre-processor software package Gambit. Auvinen [7] studied the issue by performing a CFD analysis of a ingleblade sewage pump with FINFLO

Navier-Stokes solver. The results are compared to experimental measurements provided by the pump manufacturer. In the analysis two contrasting solution schemes were utilized (time-accurate and quasi-steady methods) and their validity was assessed.

In the present study a three-dimensional numerical study of steady, turbulent and incompressible flow characteristics inside the passage between two blades of centrifugal pump impeller is presented. A finite volume method for solving Navier-Stokes equations in conical coordinate system with staggered grid arrangement is also presented

2. The Governing Equations

In order to fit an arbitrary hub and shroud surfaces shapes, the conical coordinate system of ϕ, r and θ coordinates would be used as shown in Figure (1).

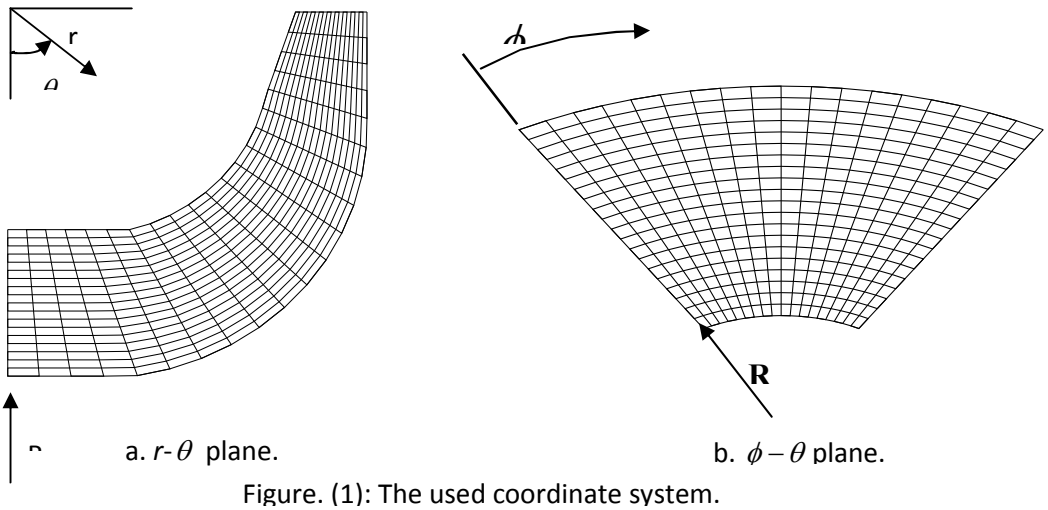

a. r-θ plane. b. $\phi - \theta$ plane.

Figure. (1): The used coordinate system.

The equations for conservation of mass and momentum for incompressible, steady and turbulent flow in each of the ϕ, r and θ directions are given below [8]:

(i) Mass Conservation .

$$\frac{1}{R}\frac{\partial}{\partial \phi}(\rho u) + \frac{1}{rR}\frac{\partial}{\partial r}(rR\ \rho v) + \frac{1}{r}\frac{\partial}{\partial \theta}(\rho w) = 0 \qquad (1)$$

(ii) Momentum Conservation .

(ϕ) – direction

$$\frac{1}{R}\frac{\partial}{\partial \phi}\left(\rho uu - \frac{\mu_{eff}}{R}\frac{\partial u}{\partial \phi}\right) + \frac{1}{rR}\frac{\partial}{\partial r}(rR\ \rho vu -$$
$$rR\ \mu_{eff}\ \frac{\partial u}{\partial r}\Big) + \frac{1}{r}\frac{\partial}{\partial \theta}\left(\rho wu - \frac{\mu_{eff}}{r}\frac{\partial u}{\partial \theta}\right) = \qquad (2)$$
$$-\frac{1}{R}\frac{\partial P}{\partial \phi} + \frac{\rho}{R}(u + 2\Omega R)(v\cos\theta - w\sin\theta)$$

(r) – direction

$$\frac{1}{R}\frac{\partial}{\partial \phi}\left(\rho uv - \frac{\mu_{eff}}{R}\frac{\partial v}{\partial \phi}\right) + \frac{1}{rR}\frac{\partial}{\partial r}(rR\ \rho vv -$$
$$rR\ \mu_{eff}\ \frac{\partial v}{\partial r}\Big) + \frac{1}{r}\frac{\partial}{\partial \theta}\left(\rho wv - \frac{\mu_{eff}}{r}\frac{\partial v}{\partial \theta}\right) = \qquad (3)$$
$$-\frac{\partial P}{\partial r} + \frac{\rho w^2}{r} - \frac{\rho\cos\theta}{R}(u + \Omega R)^2$$

(θ) – direction

$$\frac{1}{R}\frac{\partial}{\partial \phi}\left(\rho uw - \frac{\mu_{eff}}{R}\frac{\partial w}{\partial \phi}\right) + \frac{1}{rR}\frac{\partial}{\partial r}(rR\ \rho vw -$$
$$rR\ \mu_{eff}\ \frac{\partial w}{\partial r}\Big) + \frac{1}{r}\frac{\partial}{\partial \theta}\left(\rho ww - \frac{\mu_{eff}}{r}\frac{\partial w}{\partial \theta}\right) = \qquad (4)$$
$$-\frac{1}{r}\frac{\partial P}{\partial \theta} - \frac{\rho vw}{r} + \frac{\rho\sin\theta}{R}(u + \Omega R)^2$$

The effective viscosity (μ_{eff}) is taken to be the sum of the laminar viscosity (μ_L) and the turbulent viscosity (μ_t) which is determined by using the modified Prandtl's mixing length turbulence model formula, given below [8] :

$$\mu_t = \left| f\ \rho\, l^2 \right| \frac{\partial w}{\partial n} \qquad (5)$$

Where l is mixing length, n is a distance measured in the direction towards the nea- rest wall and f accounts for effects of curvature and rotation. In this paper f will be specified so as to satisfy continuity equation at the inlet and exit of the impeller passage. The value of f can be evaluated within the range (0.1-10) [8].

3. Finite Difference Formulation of the Equations

The basic of the numerical method is the conversion of the differential equations (1, 2, 3 and 4) into algebraic equations relating the value of the dependent variables at the considered grid point to the its values at the neighboring grid points. This was done by finite difference method.

After treating the governing equations by (FDM), the general form of the resultant equation can be termed as [9] :

$$a_j \Phi_j = \left(\sum_{E,W,S,N,B,F} a\Phi \right) + b \qquad (6)$$

Where Φ is the general form of the dependent variable [9].

This equation is known as a three-dimensional discretization equation. Where (a_E, a_W, a_S, a_N, a_B and a_F) are the neighboring coefficient representing the convection and diffusion terms of the mass entering the cell at its boundary surfaces, which are equal to :

$$a_E = -\rho \frac{1}{2R_j} \frac{u_e}{\Delta\phi} + \mu_{eff} \frac{1}{R_j^2 \Delta\phi^2} \quad (7a)$$

$$a_W = \rho \frac{1}{2R_j} \frac{u_w}{\Delta\phi} + \mu_{eff} \frac{1}{R_j^2 \Delta\phi^2} \quad (7b)$$

$$a_S = -\rho \frac{v_s}{2\Delta r} + \mu_{eff} \left[\frac{1}{\Delta r^2} + \frac{1}{2R_j} \frac{R_s - R_n}{\Delta r} \frac{1}{\Delta r} + \frac{1}{2r_j} \frac{1}{\Delta r} \right] \quad (7c)$$

$$a_N = \rho \frac{v_n}{2\Delta r} + \mu_{eff} \left[\frac{1}{\Delta r^2} - \frac{1}{2R_j} \frac{R_s - R_n}{\Delta r} \frac{1}{\Delta r} - \frac{1}{2r_j} \frac{1}{\Delta r} \right] \quad (7d)$$

$$a_B = -\rho \frac{1}{2r_j} \frac{w_b}{\Delta\theta} + \mu_{eff} \left[\frac{1}{r_j^2 \Delta\theta^2} + \frac{1}{2r_j} \frac{(1/r)_b - (1/r)_f}{\Delta\theta} \frac{1}{\Delta\theta} \right] \quad (7e)$$

$$a_F = \rho \frac{1}{2r_j} \frac{w_f}{\Delta\theta} + \mu_{eff} \left[\frac{1}{r_j^2 \Delta\theta^2} - \frac{1}{2r_j} \frac{(1/r)_b - (1/r)_f}{\Delta\theta} \frac{1}{\Delta\theta} \right] \quad (7f)$$

$$a_j = \left(\sum_{E,W,S,N,B,F} a \right) + b_1 \quad (7g)$$

Where the subscript (j) denotes the corresponding grid point. The small letters subscript (e, w, s, n, b and f) denote the value of the variable at the faces of the control volume. Figure (2) shows the corresponding grid point and its neighbor grid points, while Figure (3) illustrates the velocity components.

Table (1) illustrates the value of (b) for Equation (6) and the value of (b_1) for Equation (7g) for the governing equations.

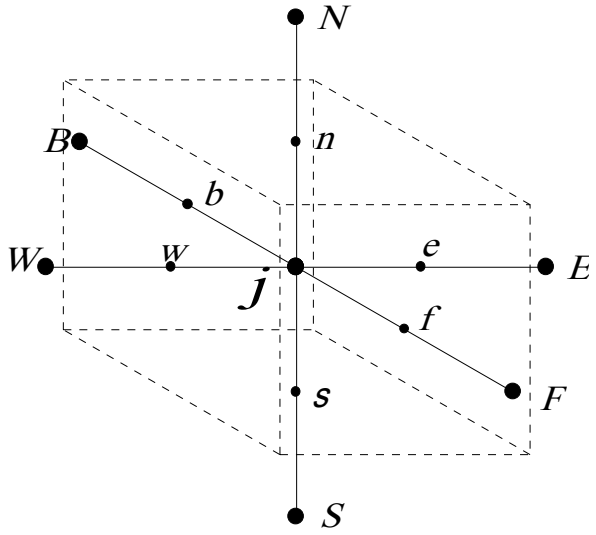

Figure (2) Typical three-dimensional control volume.

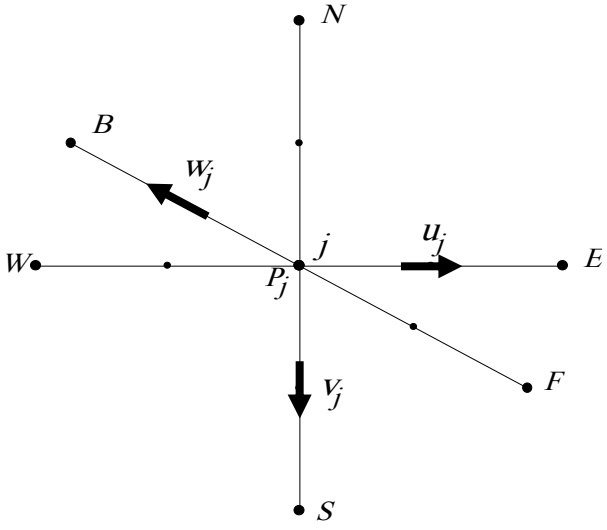

Figure (3) Velocity components.

ϕ– direction momentum equation

b_1	$\rho\left[\frac{1}{R_j}\frac{v_s+v_n}{2}\cos\theta_j-\frac{1}{R_j}\frac{w_b+w_f}{2}\sin\theta_j\right]$
b	$-\frac{1}{R_j}\frac{p_E-p_j}{\Delta\phi}+\rho\left[(v_s+v_n)\Omega\cos\theta_j-(w_b+w_f)\Omega\sin\theta_j\right]$
r – direction momentum equation	
b_1	0
b	$-\frac{p_s-p_j}{\Delta r}+\rho\left[\frac{w_j^2}{r_j}-\frac{\cos\theta_j}{R_j}(u_j+\Omega R_j)^2\right]$
θ – direction momentum equation	
b_1	$-\rho\frac{v_j}{r_j}$
b	$-\frac{1}{r_j}\frac{p_B-p_j}{\Delta\theta}+\rho\left[\frac{\sin\theta_j}{R_j}(u_j+\Omega R_j)^2\right]$

Table (1) Value of b and b_1 for Equations (6 and 7g) for governing equations.

4. Method of Solution

The first step in the solution is dividing the flow field into grid points, then the partial differential equations would be transformed into an algebraic form by finite-difference method as illustrated in the previous section. The discretized procedure of the equation is based on the power law scheme [9] and the discretized equations are solved by (TDMA) (Try Diagonal Matrix Algorithm) with under-relaxation factor 0.75 for pressure and 0.45 for velocity. The pressure and velocity are linked by the SIMPLE algorithm [9].

5. Computer Program Descriptions

A computer program in FORTRAN-90 is written to solve a set of the partial differential equations that govern the flow field. The field is divided into (19*19*21) grid points, which are distributed in an irregular, nearly orthogonal manner over the ϕ, r and θ coordinates. Figure (4) illustrates the grid point and control volume for the field.

6. Case Study

The impeller considered in this paper is the same of this used by Murakami et al., [1] which is shown in Figure (5). The operating conditions are as illustrated in Table (2).

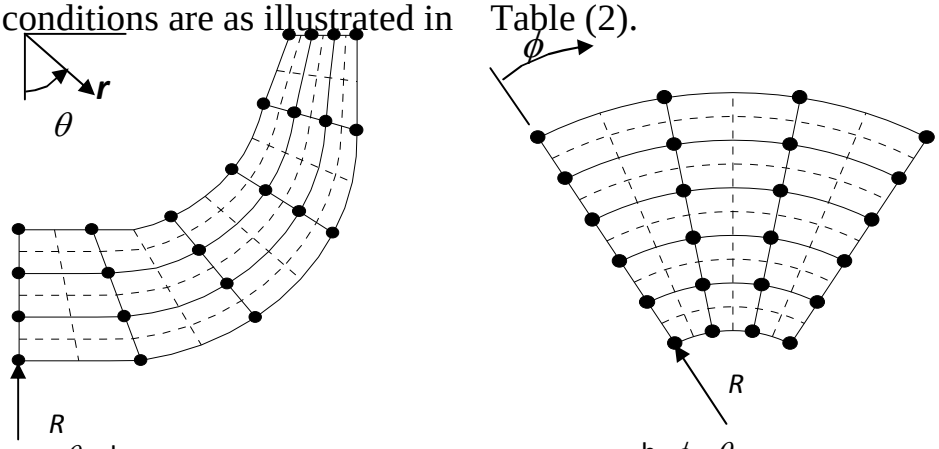

a. r-θ plane. b. $\phi - \theta$

Figure. (4): Grid and control volumes system.

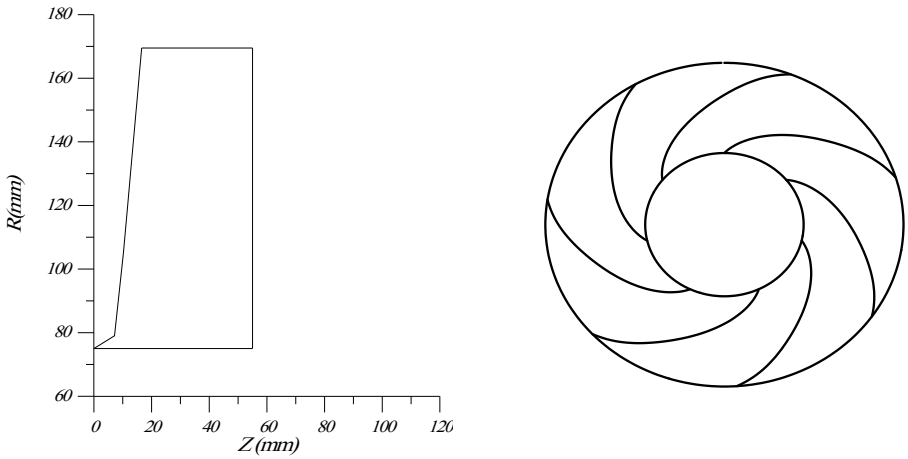

a. Meridional profile. b. Mean blade shape.

Figure. (5): Meridional profile and mean blade shape for the impeller

Operating conditions	Data

Rotational speed	400 rpm
Velocity at inlet	1 m/s
Inlet diameter	75 mm
Outlet diameter	169.5 mm
Number of blades	7
Density of fluid	1000 kg/m^3

Table (2) Operating conditions

7. Results and Discussions

The experimental results of the flow pattern through the impeller were measured by Murakami et al., [1] at two locations (at radial section r/r_o=0.7 and 0.99). These results are used to check the validity of the present method.

Figures (6 and 7) show the development of main relative velocity (w-component) profiles on blade-to-blade surfaces. Values of non-dimensional relative velocity to tip speed are plotted for three stations; near the shroud, mid way and near the hub.

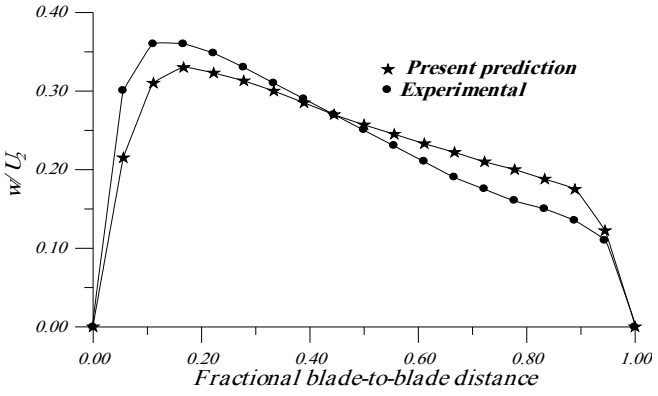

a. Near the shroud.

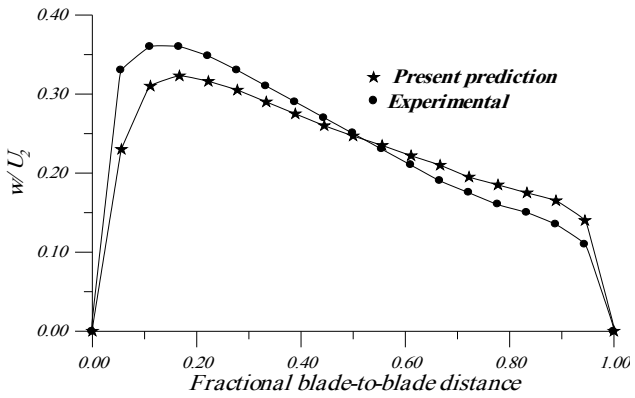

b. Mid-way.

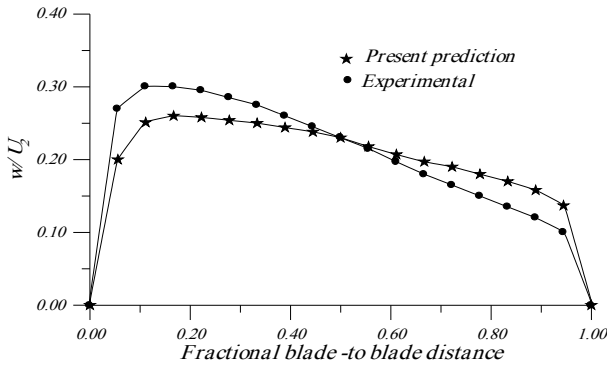

c. Near the hub.

Figure (6): Blade-to-blade relative velocity profiles at r/r_o=0.7.

A comparison between the experimental and present numerical results at r/r_o=0.7 shows acceptable agreement as illustrated in Figure (6). The relative velocity seems larger at the low-pressure side as a result of the rotation and circulation.

At exit (r/r_o=0.99), the comparison shows an acceptable agreement as shown in Figure (7). The discrepancy between the experimental and present numerical results is due to the effect of the volute casing on the flow leaving the impeller, which appears in the experimental curves.

The vector field of the relative velocity for three hub-to-shroud surfaces is presented in Figure (8). This figure shows how the flow changes its direction from axial to redial and the relative velocity seems small near the walls (hub and shroud).

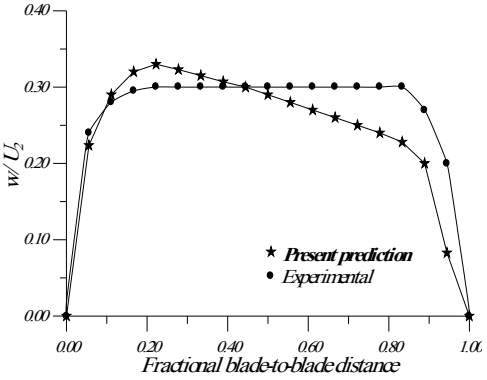

c. Near the hub.

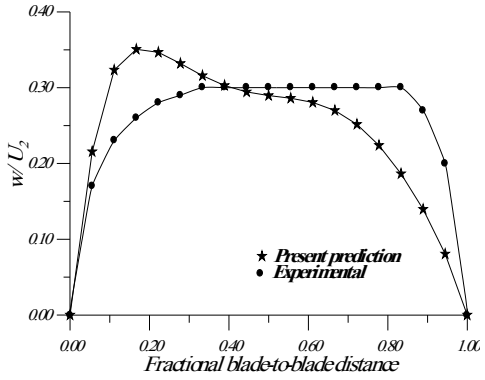

a. Near the shroud.

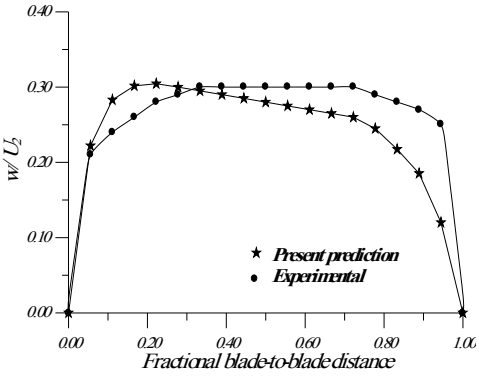

b. Mid-way.

Figure (7): Blade-to-blade relative velocity profiles at r/r_o=0.99 (Continued).

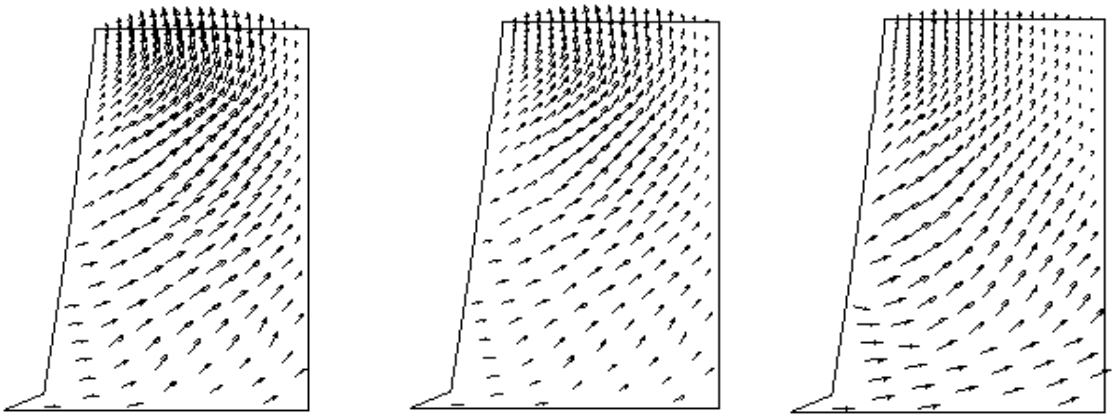

a. Near suction side. b. Mid-way. c. Near the hub.

Figure (8)Vector field of the relative velocity on hub-to-shroud stream surfaces.

Figure (9) shows the vector field of the relative velocity for three blade-to-blade surfaces. This figure shows how the flow changes its direction

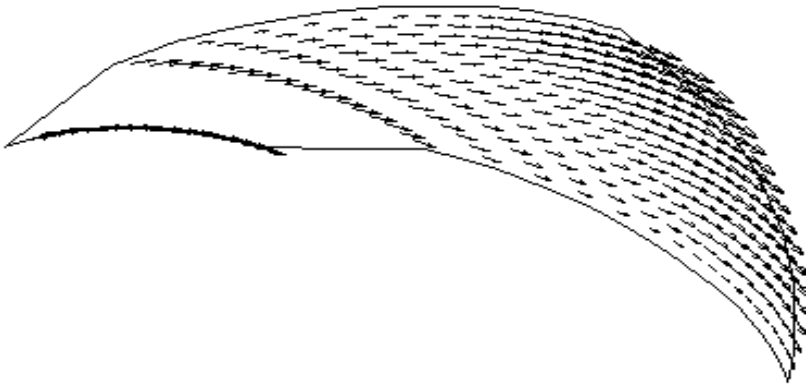

a. Near the shroud.

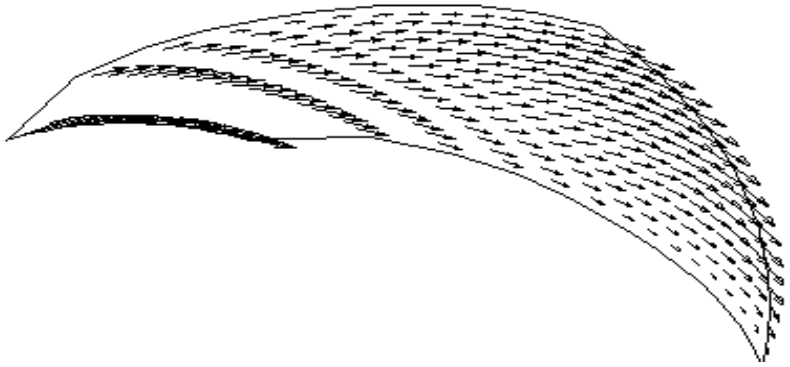

b. Mid-way.

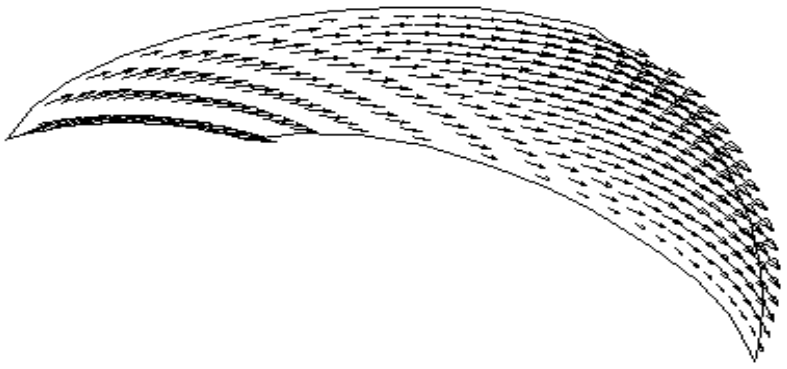

1cm : 6 m/s

c. Near the hub.

The vector field of the secondary flow on the surfaces, which are normal to the flow direction, is plotted in Figure (10). Due to the impeller rotation, the secondary flow is directed towards the pressure side. The secondary flow is very small, so the scale used to plot Figure (10) is approximately twice as that used to plot Figures (8 and 9).

The equipressure lines (coefficient of pressure head (ψ)) were drawn near the shroud surface for experimental method as shown in Figure (11), while the present numerical ones are shown in Figure (12). The comparison between the two figures shows acceptable agreement. The equipressure lines are seen to be inclined in the circumferential direction.

Shroud

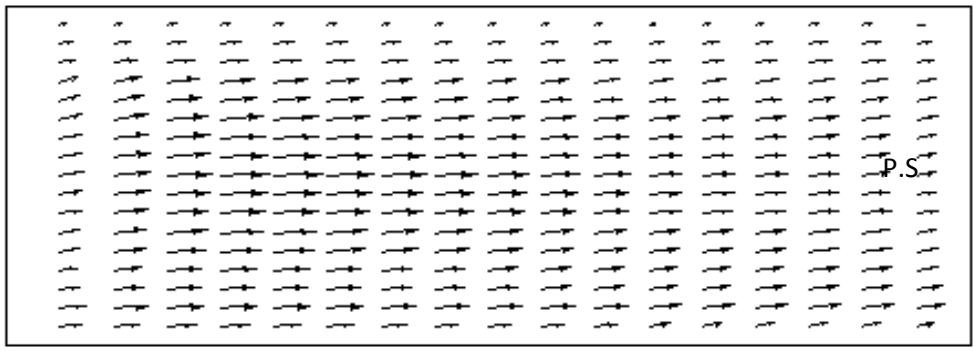

S.S

P.S

Hub

a. At radial section r/r_o=0.7 .

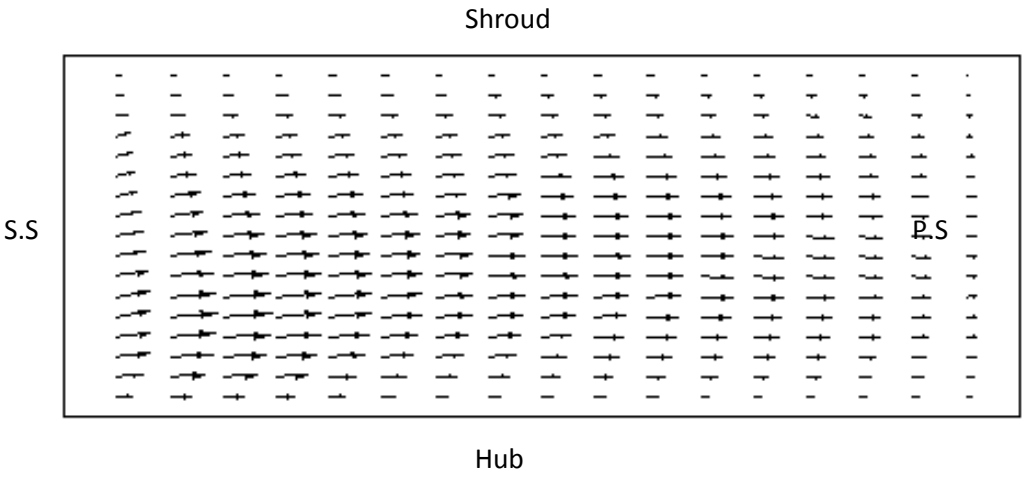

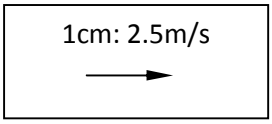

b. At radial section r/r_o=0.99

Figure (10) Vector field for the secondary flow.

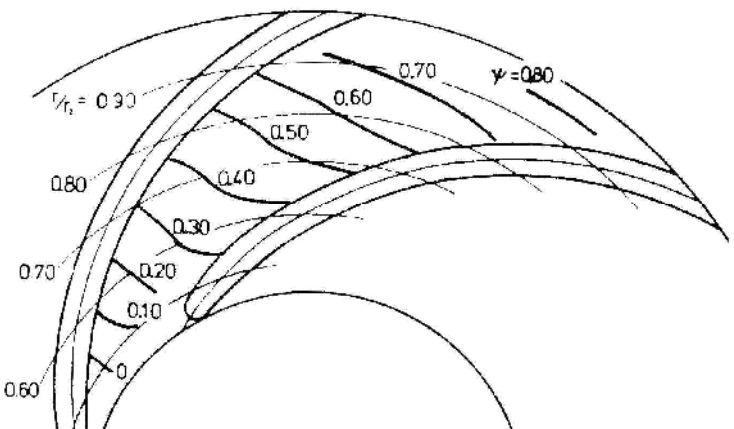

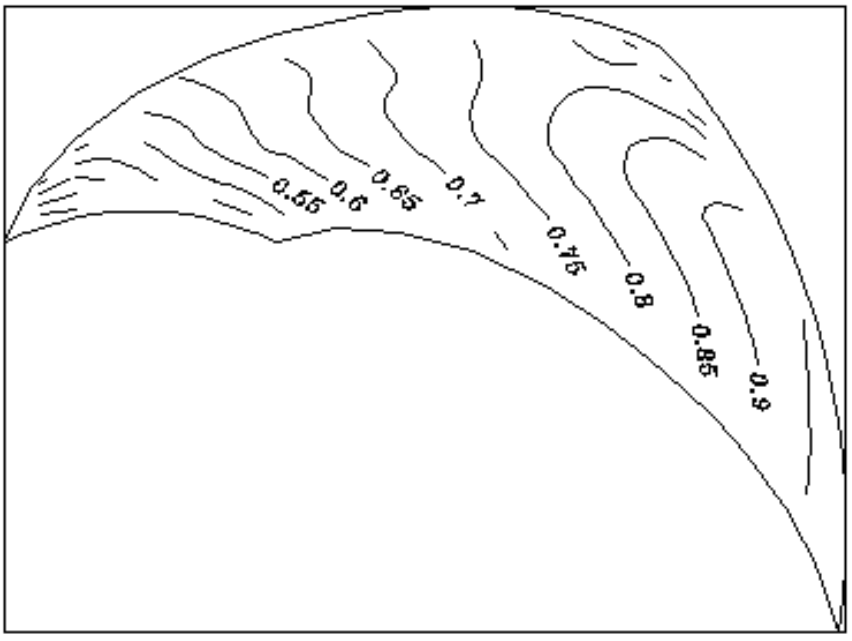

Figure (12): Pressure contour on a blade-to-blade surface for the present prediction.

8. Conclusions and Recommendations

A numerical three-dimensional, through flow calculations to predict velocity and pressure through a centrifugal pump were presented. The predicted results were in good agreement with the experimental results. For future work, the followings are suggested:

1. Reformulate the governing equations in a more usual coordinate system of x, y and z to permit solution for any general surface of revolution, by using grid generation method.
2. Develop the present turbulence model by using a two-equation turbulence model (k-ε turbulence model), and modifying it to take into account rotational and curvature effects.
3. The program could be extended and improved to predict the flow characteristics for compressor or turbine.

References

[1] Murakami, M. Kikuyama, K. and Asakura, E. , “Velocity and pressure distributions in the impeller passage of centrifugal pumps .” ASME Journal of Fluids Engineering, Vol. 102, 1980.

[2] Zhang, G. and Assanis, D. N., ” Segregated prediction of 3-D compressible subsonic fluid flows using collocated grids.”, Numerical Heat Transfer, Part A, 29 : 757-775, 1996.

[3] Polititis, E. S. and Giannakoglou, K. C. A., ” A pressure-based algorithm for high-speed turbomachinery flows.” , International Journal for Numerical Methods in Fluids, Vol. 25, No.1 , 63-80, 1997.

[4] Wang, Y. and Komori, S., ” Simulation of the subsonic flow in a high-speed centrifugal compressor impeller by the pressure based method.” Proc. Inst. Mech. Engrs., Vol. 212, part A, 269-287, 1998.

[5] Hofmann M. and Stoffel B., " Experimental and numerical studies on a centrifugal pump with 2D-curved blades in cavitating condition." Laboratory for Turbomachinery and Fluid Power, Darmstadt University of Technology, Germany, CAV2001

[6] Mununga, L. , Hourigan, K. and Thompson, M. " Numerical study of the effect of blade size on pumping effectiveness of a paddle impeller in an unbaffled mixing vessel." Third International Conference on CFD in the Minerals and Process Industries, CSIRO Melbourne, Australia, December 2003.

[7] Auvinen, M. " Computational analysis of a single-blade sewage pump with FINFLO." Helsinki University of Technology Laboratory of Applied Thermodynamics, CFD Group, 6th March 2006.

[8] Malin ,M.R., Rosten , H. I. and Tatchell, D.G. “ Three-dimensional computations of flows in centrifugal pumps and compressors.” Presented by “Performance predication of centrifugal pumps and compressors.” Copyright by ASME, pp33-45, 1979.

[9] Patankar ,S. V. , “Numerical heat transfer and fluid flow .” McGraw–Hill Company, Now York, 1980.